

Observational Constraints on Dark Energy Models with Λ as an Equilibrium Point

Andronikos Paliathanasis^{1,2,3,4,*}

¹*Department of Mathematics, Faculty of Applied Sciences,
Durban University of Technology, Durban 4000, South Africa*

²*Centre for Space Research, North-West University, Potchefstroom 2520, South Africa*

³*Departamento de Matemáticas, Universidad Católica del Norte,
Avda. Angamos 0610, Casilla 1280 Antofagasta, Chile*

⁴*National Institute for Theoretical and Computational Sciences (NITheCS), South Africa.*

We investigate a dynamical reconstruction of the dark energy equation of state parameter by assuming that it satisfies a law of motion described by an autonomous second-order differential equation, with the limit of the cosmological constant as an equilibrium point. We determine the asymptotic solutions of this equation and use them to construct two families of parametric dark energy models, employing both linear and logarithmic parametrization with respect to the scale factor. We perform observational constraints by using the Supernova, the Cosmic Chronometers and the Baryon Acoustic Oscillations of DESI DR2. The constraint parameters are directly related with the initial value problem for the law of motion and its algebraic properties. The analysis shows that most of the models fit the observational data well with a preference to the models of the logarithmic parametrization. Furthermore, we introduce a new class of models as generalizations of the CPL model, for which the equilibrium point is a constant value rather than the cosmological constant. These models fit the data in a similar or better way to the CPL and the Λ CDM cosmological models.

PACS numbers:

Keywords: Dynamical dark energy; Observational Constraints; Parametric equation of state.

1. INTRODUCTION

Recent cosmological data indicate that currently the universe is under an acceleration phase [1–5]. Within the framework of General Relativity, this late-time expansion is attributed to the dark energy fluid [6–8], with a negative pressure component which provides repulsive-gravitational forces within the universe. Nevertheless, the lack of a fundamental physical theory explaining the mechanism behind cosmic acceleration has led to the dark energy problem, for which a wide range of cosmological scenarios and theories have been proposed for the description of the cosmic acceleration.

The introduction of the cosmological constant Λ within the Einstein-Hilbert action is the simplest solution for the dark energy problem. The cosmological constant, leading to the Λ CDM universe, has the minimum number of free degrees of freedom and it can explain the late-time acceleration phase. However, it suffers from mayor problems such as the fine tuning problem and the coincidence problem [9–11]. Recently, Λ CDM is challenged more due to the cosmological tensions [12–14]. Because of these problems, cosmologists have introduced a plethora of theoretical [15–29] and phenomenological proposals [30–35] to address the dark energy problem.

The determination of the equation of state parameter for the dark energy component can provide crucial insights into the nature of this exotic fluid source. Dynamical dark energy models with a time-varying equation of state parameter $w(a)$ have been introduced to explain cosmological observations. The Chevallier, Polarski and Linder [36, 37] (CPL) parametrization is the simplest varying dark energy model, introducing two degrees of freedom. The CPL model helps to determine how distinct a given dark energy model is from the cosmological constant [38–41]. Due to the limitations of the CPL model, various alternative dark energy models have been proposed over the past two decades. For more details, we refer the reader to [59–72] and the references therein. The recent Baryon Acoustic Oscillations of DESI DR2 data indicate a preference for dynamical dark energy models over the Λ CDM model. The family of $w_0 w_a$ CDM [42–44]. This data set has been used to examined various theoretical models which lead to a dynamical dark energy [45–58].

In this study, we focus upon a dynamical reconstruction of the dark energy equation of state parameter. Specifically, we assume that the equation of state parameter satisfies a law of motion, meaning that it is governed by a differential equation, with the requirement that the cosmological constant limit exists as an equilibrium point at the present time.

*Electronic address: anpaliat@phys.uoa.gr

We determine all possible functional forms for the asymptotic solution of this dynamical dark energy law of motion near the equilibrium point, allowing us to construct families of parametric dark energy models.

The parametrization of this law of motion is significant, as it provides information about the nature of dark energy. We employ two types of parametrization. Firstly, we consider a parametrization that is linear in the scale factor, leading to exponential forms of the dark energy equation of state parameter, with or without oscillatory components. These models exhibit an approximate behavior similar to that of the CPL model. As a second parametrization, we assume that the independent variable of this law of motion follows a logarithmic function. This parametrization has a theoretical foundation, as it can relate the evolution of dark energy parameters to the dynamics of scalar fields [73–75], modified theories of gravity [76, 77] or interacting models [78] and others. The dynamical dark energy models related to this parametrization have polynomial expression.

By using the above parametrization, we constructed two families of models and applied observational constraints for the late universe to determine the free parameters and assess the validity of the reconstruction approach. From the data analysis, we found that most models fit the cosmological data well, in a manner similar to the Λ CDM model. However, due to the larger number of free parameters, Λ CDM remains statistically preferred. Nonetheless, two models constructed using the logarithmic parametrization were found to be statistically indistinguishable from Λ CDM. Furthermore, we found that models with oscillatory components and decaying behavior are not favored by the data.

Finally, we introduced a new class of models that can be seen as generalizations of the CPL model, where the equilibrium point of the differential equation is not the cosmological constant but a constant parameter, introducing an additional degree of freedom within the models. These new models fit the data as well as or better than the CPL model and are statistically indistinguishable from it. This analysis provides important insights into the law of motion that dark energy satisfies and its fundamental nature. The structure of the paper is as follows.

In Section 2 we introduce the cosmological model of our consideration, which is that of spatially flat FLRW geometry in which the dark energy has a dynamical equation of state parameter $w(a)$. In Section 3 we assume that $w(a)$ is given by a nonlinear differential equation $F(w_d, w'_d, w''_d) = 0$ in which the limit of the cosmological constant Λ exists as an equilibrium point at the present time. We employ the theory of dynamical systems and explore the functional forms of $w(a)$ as it reaches the equilibrium point with the value -1 .

In particular, we consider that $w(a)$ follows from a second-order differential equation $F(w_d, w'_d, w''_d) = 0$ and we write three generic functional forms of $w(a)$ related to the algebraic properties of the differential equation $F(w_d, w'_d, w''_d) = 0$. These models depend upon four free parameters, except for the case for which the differential equation F is of first order and there are two parameters. The determination of the free parameters of the models leads to important information and constraints for the original physical law which describes the dark energy equation of state parameter. However, from the structure of the parameter space for the free variables, we discuss the possible correlation of the free parameters. Therefore, we end with eight dark energy models that depend upon one or two free parameters.

In Section 4 we introduce the observational data applied in this work. In particular, we consider the Pantheon+ Supernova data, the Cosmic Chronometers and the Baryonic Acoustic Oscillators. The results from the observational constraints of the proposed dynamical dark energy models are presented in Section 5. Finally, in Section 6, we discuss possible extension of this approach and we draw our conclusions.

2. COSMOLOGICAL FRAMEWORK

We assume that the physical space is described by a four-dimensional Riemannian manifold with a metric tensor that is both isotropic and homogeneous, as described by the spatially flat FLRW line element

$$ds^2 = -dt^2 + a^2(t)(dx^2 + dy^2 + dz^2), \quad (1)$$

where $a(t)$ is the scale factor which describes the radius of the three-dimensional hypersurface.

Let $u^\mu = \delta^\mu_t$, with $u^\mu u_\mu = -1$, be the comoving observer. Let $T_{\mu\nu}$ be the energy momentum tensor for the cosmic fluid. Within the $1 + 3$ decomposition we can define the observable energy density, the pressure, the heat flux and the stress tensor as follows

$$\rho = T_{\mu\nu} u^\mu u^\nu, \quad (2)$$

$$p = \frac{1}{3} T_{\mu\nu} h^{\mu\nu}, \quad (3)$$

$$q_\mu = T_{\lambda\nu} h^{\lambda\nu} u_\mu, \quad (4)$$

$$\pi_{\mu\nu} = T_{\lambda\sigma} h_\mu^\lambda h_\nu^\lambda - p h_{\mu\nu}. \quad (5)$$

in which $h_{\mu\nu} = g_{\mu\nu} + u_\mu u_\nu$ is the projective tensor. Hence, the energy momentum tensor in terms of these latter physical quantities is

$$T_{\mu\nu} = \rho u_\mu u_\nu + p h_{\mu\nu} + 2q_{(\mu} u_{\nu)} + \pi_{\mu\nu}. \quad (6)$$

For the gravitational model, we consider Einstein's General Relativity. The gravitational field equations are given by

$$R_{\mu\nu} - \frac{1}{2} R g_{\mu\nu} = T_{\mu\nu}, \quad (7)$$

where, for the line element (1) and the comoving observer, it follows that

$$3H^2 = \rho, \quad (8)$$

$$2\dot{H} + 3H^2 = p \quad (9)$$

and $q_\mu = 0$, $\pi_{\mu\nu} = 0$, where $H = \frac{\dot{a}}{a}$ is the Hubble function and it is related to the expansion rate $\theta = u^\mu_{;\mu}$ as follows $\theta = 3H$.

Within the FLRW geometry, the cosmic fluid is described by a perfect fluid. Moreover, the Bianchi identity leads to the conservation law for the fluid source:

$$\dot{\rho} + 3H(\rho + p) = 0. \quad (10)$$

We assume that the cosmological fluid consists of the following components:

$$\rho = \rho_r + \rho_b + \rho_{dm} + \rho_d, \quad (11)$$

where ρ_r notes for the radiation, $p_r = \frac{1}{3}\rho_r$, ρ_b is the pressureless baryonic matter $p_b = 0$, ρ_m is the cold dark matter, $p_m = 0$, and ρ_d marks as the energy density for the dark energy source, $p_d = w_d \rho_d$. Therefore, the pressure component of the cosmological fluid

$$p = \frac{1}{3}\rho_r + w_d \rho_d. \quad (12)$$

We substitute (11) and (12) into the continuity equation (10). It follows that

$$(\dot{\rho}_r + 4H\rho_r) + \dot{\rho}_b + \dot{\rho}_{dm} + (\dot{\rho}_d + 3(1 + w_d)H\rho_d) = 0. \quad (13)$$

Furthermore, if there is no energy transfer between the four fluids, it follows that

$$\rho_r = \rho_{r,0} \left(\frac{a}{a_0}\right)^{-4}, \quad \rho_b = \rho_{b,0} \left(\frac{a}{a_0}\right)^{-3}, \quad \rho_{dm} = \rho_{dm,0} \left(\frac{a}{a_0}\right)^{-3} \quad (14)$$

and

$$\rho_d = \rho_{d,0} \exp\left(-3 \int_a^{a_0} \frac{1 + w_d(\alpha)}{\alpha} d\alpha\right). \quad (15)$$

Parameters $\rho_{I,0}$ are integration constants and define the energy density of the corresponding fluids at the present $\frac{a}{a_0} = 1$.

With the use of these expressions, from equation (8) it follows that

$$H(a) = H_0 \sqrt{\Omega_{r0} \left(\frac{a}{a_0}\right)^{-3} + \Omega_{b0} \left(\frac{a}{a_0}\right)^{-3} + \Omega_{dm0} \left(\frac{a}{a_0}\right)^{-3} + \Omega_{d0} \exp\left(-3 \int_a^a \frac{1 + w_d(\alpha)}{\alpha} d\alpha\right)}, \quad (16)$$

in which H_0 is the value of the Hubble function at the present and $\Omega_{I,0} = \frac{\rho_{I,0}}{3H_0^2}$.

From expression (16) we determine the algebraic equation

$$\Omega_{r0} + \Omega_{b0} + \Omega_{dm0} + \Omega_{b0} = 1. \quad (17)$$

The choice of the dark energy model determines the cosmic evolution of the physical parameters. Simultaneously, the selection of the function $w_d(a)$ is crucial for defining the cosmological model.

When the dark energy is described by the cosmological constant, it follows that $w_d(a) = -1$, from which the Λ CDM model is recovered. Expression (16) is

$$H(a) = H_0 \sqrt{\Omega_{r0} \left(\frac{a}{a_0}\right)^{-3} + \Omega_{b0} \left(\frac{a}{a_0}\right)^{-3} + \Omega_{dm0} \left(\frac{a}{a_0}\right)^{-3} + \Omega_{\Lambda 0}}. \quad (18)$$

On the other hand, for a dark energy fluid with constant equation of state parameter $w_d(a) = w_0$, the Hubble function is

$$H(a) = H_0 \sqrt{\Omega_{r0} \left(\frac{a}{a_0}\right)^{-3} + \Omega_{b0} \left(\frac{a}{a_0}\right)^{-3} + \Omega_{dm0} \left(\frac{a}{a_0}\right)^{-3} + \Omega_{d0} a^{-3(1+w_0)}}. \quad (19)$$

The definition of the equation of state parameter, $w_d(a)$, for the dark energy can follow from a theoretical background or a phenomenological approach. Scalar fields or modified theories of gravity have been introduced to explain the nature of dark energy and to construct dark energy fluids that can account for cosmological observations. On the other hand, within the phenomenological framework, parametric dark energy models with specific functions, $w_d(a)$, have been introduced in the literature as an attempt to understand the effects of $w_d(a)$ in the analysis of cosmological parameters.

The Chevallier-Polarski-Linder (CPL) model is the simplest parametrization of the $w_d(a)$, where $w_d(a)$ is a linear function such that $w_d(a) = w_0 + w_a \left(1 - \left(\frac{a}{a_0}\right)\right)$ or, equivalently,

$$w_d^{CPL}(z) = w_0 + w_a \left(\frac{z}{1+z}\right), \quad (20)$$

where $1+z = \frac{1}{a}$ is the redshift parameter. The CPL parametrization provides the two limits. At the present $w_d(z \rightarrow 0) = w_0$, while in the past $w_d(z \rightarrow +\infty) = w_0 + w_a$.

The CPL model can be seen as the first-order approximation of the exponential parametric dark energy model $w_d(a) = w_0 + w_a (e^{1-a} - 1)$ or, equivalently [65],

$$w_d^{Exp}(z) = w_0 + w_a e^{\frac{z}{1+z}}. \quad (21)$$

Indeed, if we expand the latter in terms of the Taylor expansion, it follows that [66]

$$w_d^{Exp}(z) = w_0 + w_a \left(\sum_{n=1}^{\infty} \left[\frac{1}{n!} \left(\frac{z}{1+z} \right)^n \right] \right), \quad (22)$$

where in the first order approximation, for $z \ll 1$, it follows that $w_d^{Exp}(z) \simeq w_d^{CPL}(z)$.

Dark energy models with oscillating terms [67–71] have been proposed in the literature, see, for instance, the model [71]

$$w_d^{Osc}(z) = -1 + w_a \frac{z}{1+z^2} \sin(w_b z), \quad (23)$$

which has the Λ limit at the present $w_d^{Osc}(z \rightarrow 0) = -1$ and in the past, $w_d^{Osc}(z \rightarrow +\infty) = -1$. In the first order approximation for low values of the redshift it follows that $w_d^{Osc}(z) \simeq w_d^{CPL}(z, w_0 \rightarrow -1)$, which is that of the CPL model with $w_0 = -1$.

3. DYNAMICAL DARK ENERGY WITH Λ AS AN EQUILIBRIUM POINT

There is a “zoology” of proposed models in the literature as we discussed in the Introduction. However, in this work, we consider that the dark energy equation of state parameter $w_d(a)$ satisfies an autonomous differential equation of the form $F(w_d, w'_d, w''_d, \dots) = 0$, where w'_d denotes the derivative with respect to the scale factor, such that $w'_d = \frac{dw_d(a)}{d\chi(a)}$, where $\chi(a)$ is a smooth, continuous function. This approach is motivated by certain scalar field models that have been used to describe inflation; see, for instance, [79, 80].

Physics laws are often described by second-order differential equations. Inspired by this, we assume that the differential equation $F(w_d, w'_d, w''_d) = 0$ is of second order and takes the form

$$w''_d = W(w_d, w'_d), \quad (24)$$

where $w_d = -1$ is an equilibrium point, meaning that $W(w_d, w'_d)|_{w_d \rightarrow -1} = 0$, ensuring that the equilibrium constant is well-defined.

In this work we do not define explicitly the differential equation that the equation of state parameter satisfies. But we try to reconstruct the solution of the equation of state parameter near to the equilibrium point. For second-order theories, like quintessence, or phantom scalar field theories, the equation that $w_d(\chi(a))$ satisfies is a first-order differential equation. On the other hand, for higher-order theories of gravity the order of differential equation is higher.

We write equation (24) in the equivalent form

$$w'_d = P_w, \quad P'_w = W(w_d, P_w) \quad (25)$$

and assume that the equilibrium $Q = (w_d(Q), P_w(Q))$ has components $Q = (-1, P_w^0)$. Then around the stationary point, the asymptotic solution for the equation of state parameter is

$$w_d(a) = -1 + w_d^1 e^{-\Delta_+(\chi(a) - \chi(a_0))} + w_d^2 e^{-\Delta_-(\chi(a) - \chi(a_0))} + c, \quad (26)$$

in which w_d^1 and w_d^2 are two constants of integration and

$$\Delta_{\pm} = \frac{1}{2} \left[\left(\frac{\partial W}{\partial P_w} \right) \pm \sqrt{\left(\frac{\partial W}{\partial P_w} \right)^2 + 4 \left(\frac{\partial W}{\partial w_d} \right)} \right]_{(w_d, P_w) \rightarrow (-1, P_w^0)}. \quad (27)$$

Constant c has been added, such that at the equilibrium point at the present time $w_d(a_0) = -1$. Its value depends upon the function $\chi(a)$. Indeed, for $\chi = \ln\left(\frac{a}{a_0}\right)$, it is easy to see that $c = 0$.

We consider the following case three cases for the value of the determinant at the equilibrium point, (i) $\left[\left(\frac{\partial W}{\partial P_w} \right)^2 + 4 \left(\frac{\partial W}{\partial w_d} \right) \right] = 0$, (ii) $\left(\frac{\partial W}{\partial P_w} \right)^2 + 4 \left(\frac{\partial W}{\partial w_d} \right) > 0$ and (iii) $\left(\frac{\partial W}{\partial P_w} \right)^2 + 4 \left(\frac{\partial W}{\partial w_d} \right) < 0$.

When the two roots Δ_+ and Δ_- are equal, the asymptotic solution around the equilibrium point is

$$w_d(a) = -1 + w_d^1 e^{-w_a(\chi(a) - \chi(a_0))}, \quad (28)$$

where $w_a = \Delta_+ = \Delta_-$.

For the second case, in which the two roots are real, it follows that the asymptotic solution around the equilibrium point Q is

$$w_d(a) = -1 + w_d^1 \exp[-w_a(\chi(a) - \chi(a_0))] + w_d^2 \exp[-w_b(\chi(a) - \chi(a_0))] + c, \quad (29)$$

with $w_a = \Delta_+$ and $w_b = \Delta_-$.

Finally, when the two eigenvalues are complex, the asymptotic solution is expressed as

$$w_d(a) = -1 + w_d^1 \exp(-w_a(\chi(a) - \chi(a_0))) \sin[w_b(\chi(a) - \chi(a_0))] + w_d^2 \exp[-(w_a(\chi(a) - \chi(a_0)))] \cos[w_b(\chi(a) - \chi(a_0))] + c, \quad (30)$$

where now $w_a = \text{Re}(\Delta_+) = \text{Re}(\Delta_-)$ and $w_b = \text{Im}(\Delta_+) = \text{Im}(\Delta_-)$. For a geometric interpretation of the stationary points we refer the reader in [81].

The requirement that the Λ CDM model be a future attractor implies that the parameter w_a must always be positive,

i.e., $w_a > 0$. In the second case, the additional condition $w_b > 0$ must also hold. On the other hand, when the real parts of the eigenvalues are positive, the Λ CDM model behaves as a source. When the real parts of both eigenvalues are zero, the equilibrium point is a center, and the asymptotic solution for the equation of state parameter oscillates around the value -1 .

These solutions describe the asymptotic behavior near equilibrium points. However, in the following, we use them as motivation to define parametric dark energy models.

At this point, it is important to note that, if the parametric dark energy equation of state parameter $w_d(a)$ were described by a first-order differential equation $F(w_d, w'_d) = 0$, then only the asymptotic behavior given by (28) could be constructed. In contrast, for higher-order differential equations, the number of eigenvalues increases, thereby introducing additional degrees of freedom.

Dynamical dark energy models with the above asymptotic behaviours can be easily reconstructed in single- and multi- scalar field cosmological models [73–75].

3.1. Linear function $\chi(a) = \frac{a}{a_0}$.

Consider now the linear function $\chi(a) = \frac{a}{a_0}$, where $\chi(1) = 1$. We define the three parametric dark energy models

$$w^I(z) = -1 + w_d^1 (\exp(w_a Z) - 1), \quad (31)$$

$$w^{II}(z) = -1 + w_d^1 (\exp(w_a Z) - 1) + w_d^2 (\exp(w_b Z) - 1), \quad (32)$$

and

$$w^{III}(z) = -1 + w_d^1 [\exp(w_a Z) \sin(w_b Z + w_c) - \sin(w_c)]. \quad (33)$$

with $Z = \frac{z}{1+z}$ and parameter c has been defined. Parameter Z takes values within the range $[0, 1]$, where 0 corresponds to the present value and 1 to the limit $a \rightarrow 0$.

At the present, i.e. $Z \ll 0$, the three models takes the form of the CPL model for $w_0 = -1$, that is,

$$w^I(z \rightarrow 0^+) \simeq -1 + (w_d^1 w_a) Z, \quad (34)$$

$$w^{II}(z \rightarrow 0^+) \simeq -1 + (w_d^1 w_a + w_d^2 w_b) Z, \quad (35)$$

$$w^{III}(z \rightarrow 0^+) \simeq -1 + (w_d^1 (w_b \sin(w_c) - \sin(w_c))) Z. \quad (36)$$

In the limit where $Z \rightarrow 1$, the equation of state parameters gives the values

$$w^I(z \rightarrow +\infty) \simeq -1 + w_d^1 (\exp(w_a) - 1), \quad (37)$$

$$w^{II}(z \rightarrow +\infty) \simeq -1 + w_d^1 (\exp(w_a) - 1) + w_d^2 (\exp(w_b) - 1), \quad (38)$$

$$w^{III}(z \rightarrow +\infty) \simeq -1 + w_d^1 [\sin(w_b + w_c) - \sin(w_c)]. \quad (39)$$

We remark that for $w_a = 1$, function $w^I(z)$ recovers the exponential parametric dark energy model studied in [66].

3.2. Logarithmic function $\chi(a) = \ln\left(\frac{a}{a_0}\right)$

A second set of common parametrization is the logarithmic function $\chi(a) = \ln\left(\frac{a}{a_0}\right)$. This choice follows naturally within the Hubble normalization [73], which is frequently applied in the study of the dynamics of gravitational field equations [73–76, 78].

Within the logarithmic parametrization we define the parametric dark energy models

$$w^{IV}(z) = -1 + w_d^1 Z^{w_a}, \quad (40)$$

$$w^V(z) = -1 + w_d^1 Z^{w_a} + w_d^2 Z^{w_b}, \quad (41)$$

and

$$w^{VI}(z) = -1 + w_d^1 [Z^{w_a} \sin(w_b Z + w_c) - \sin(w_c)]. \quad (42)$$

In this formulation, in order the models to be well defined, it is necessary that $w_a, w_b > 0$, while the CPL limit is recovered only in the models w^{IV} and w^{VI} for $w_a = 1$.

On the other hand, for $Z = 1$, the parametric functions $w^{IV}(z \rightarrow +\infty)$ and $w^V(z \rightarrow +\infty)$ have the limit -1 , while function w^{VI} gives the value

$$w^{VI}(z \rightarrow +\infty) = -1 + w_d^1 (\sin(w_b + w_c) - \sin(w_c)). \quad (43)$$

The parametric model $w^{IV}(z)$ was previously introduced in [82] and is known as the nCPL model, where n refers to the power of w_a . Observational analysis using the Union 2.1 dataset indicated a preference for high values of the parameter n . In this work, we will investigate whether this preference persists with more recent cosmological data.

We note that the parameters w_a and w_b explicitly depend on the underlying theoretical framework, specifically on the differential equations that govern $w_d(a)$. However, the parameters w_d^1 and w_d^2 depend solely on the initial conditions.

3.3. Parametric space

We discuss the parametric space for the free variables that we shall use within the analysis for the comparison to the observation data. Parametric model $w^I(z)$ depends on two parameters w_d^1 and w_a , however, for small redshift we found that the two parameters are degenerate. Indeed, in terms of statistics it will not be possible to constant these two parameters. The same discussion hold and for models $w^{II}(z)$ and $w^{III}(z)$. In Fig. 1 we present the qualitative evolution of parametric models $w^I(z)$, and $w^{II}(z)$ from where we observe that for small z , parameters are related as $w_a \sim \frac{1}{w_d^1}$ and $w_b \sim \frac{1}{w_d^2}$.

If in model $w^I(z)$ we assume $w_a = 1$, then we recover the model studied in [66]. In contrary, in this study we will reduce the parametric space by assuming $w_d^1 = \pm 1$ in $w^I(z)$ and $w_d^1 = -w_d^2 = 1$ in $w^{II}(z)$; that is, we end with the following dynamical dark energy equation of state parameters

$$\begin{aligned} w_+^I(z) &= -1 + e^{w_a Z} - 1, \\ w_-^I(z) &= -1 - (e^{w_a Z} - 1), \\ w^{II}(z) &= -1 + \sinh(w_a Z). \end{aligned}$$

In $w^{II}(z)$ we have assumed that w_d^1, w_d^2 have different signs in order to avoid any degeneration on the indices.

For model $w^{III}(z)$, and parameter w_c we consider the extreme limit $w_c = 0$, thus

$$w^{III}(z) = -1 + \exp(w_a Z) \sin(w_b Z). \quad (44)$$

This model allows can change sign.

We conclude that models $w^I(z)$, $w^{II}(z)$ depend on one parameter, namely w_a , and model $w^{III}(z)$ on two parameters, that is, w_a and w_b . Although in the first-order approximation of $w^{III}(z)$, parameters w_a, w_b are independent, this is not true in the higher-order approximation. As we shall see later, a correlation exists between these two parameters.

For the second family of parametric models $w^{IV}(z)$, $w^V(z)$ parameters (w_d^1, w_a) and (w_d^2, w_b) maybe are not related explicitly as before for small values of redshifts z . Nevertheless, for small values of z , as w_a increases \uparrow , the term $Z^{w_a} \downarrow$. Then, if $w_d^1 \uparrow$, the product changes very slowly. These variables are degenerate for small redshifts.

Therefore we introduce the following models

$$w_+^{IV}(z) = -1 + Z^{w_a}, \quad (45)$$

$$w_-^{IV}(z) = -1 - Z^{w_a}, \quad (46)$$

$$w^V(z) = -1 + Z^{w_a} - Z^{w_b}, \quad (47)$$

where again for model $w^V(z)$ we assume that the constants of integration related to the initial conditions to have different signs.

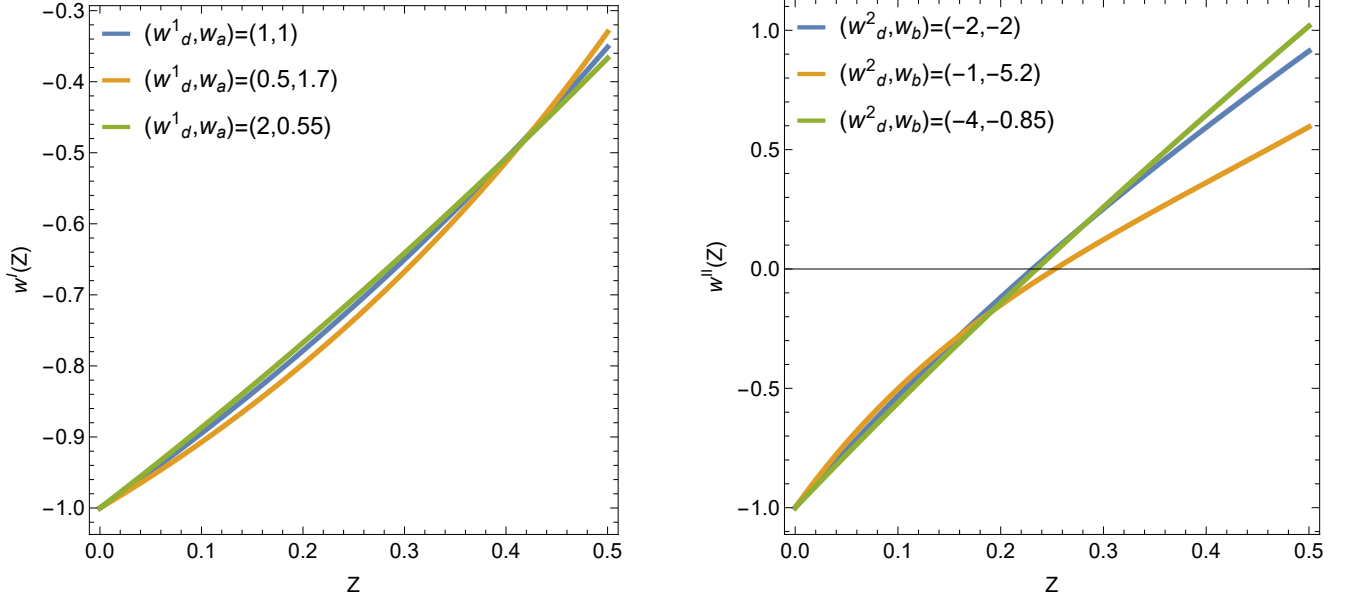


FIG. 1: Qualitative evolution of $w^I(z; w_d^1, w_a)$ (Left Fig.) and $w^{II}(z; w_d^1, w_a, w_d^2, w_b)$ (Right Fig.) for different values of the parameters. We observe that for small Z the sets of parameters (w_d^1, w_a) and (w_d^2, w_b) are degenerate.

TABLE I: Dynamical Dark Energy Models

Model	Parameters	Function $\left(Z = \frac{z}{1+z}\right)$
$w_+^I(z)$	w_a	$-1 + (e^{w_a Z} - 1)$
$w_-^I(z)$	w_a	$-1 - (e^{w_a Z} - 1)$
$w^{II}(z)$	w_a	$-1 + \sinh(w_a Z)$
$w^{III}(z)$	w_a, w_b	$-1 + \exp(w_a Z) \sin(w_b Z)$
$w_+^{IV}(z)$	w_a	$-1 + Z^{w_a}$
$w_-^{IV}(z)$	w_a	$-1 - Z^{w_a}$
$w^V(z)$	w_a, w_b	$-1 + Z^{w_a} - Z^{w_b}$
$w^{VI}(z)$	w_a, w_b	$-1 + Z^{w_a} \sin(w_b Z)$

Finally, from the generic function of $w^{VI}(z)$, similarly as above we assume $w_c = 0$. We end up with the parametric dark energy model

$$w_0^{VI}(z) = -1 + Z^{w_a} \sin(w_b Z). \quad (48)$$

The dynamical dark energy models studied in this work are summarized in Table I.

4. OBSERVATIONAL DATA

For our analysis, in order to determine the cosmological parameters, we make use of three background datasets: the Pantheon+ Type Ia supernova data (SN), the Cosmic Chronometers (CC) and the Baryonic Acoustic Oscillations (BAO) data.

- (SN) The Pantheon+ dataset¹ comprises 1701 light curves of 1550 spectroscopically confirmed supernova events within the range $10^{-3} < z < 2.27$ [87]. The data provides the distance modulus μ^{obs} at observed redshifts z . The theoretical distance modulus is constructed as follows $\mu^{th} = 5 \log D_L + 25$, where D_L is the luminosity distance defined by the Hubble functions from the expression $D_L = c(1+z) \int \frac{dz}{H(z)}$.
- (CC) For the Cosmic Chronometers we use 31 direct measurements of the Hubble parameter across redshifts in the range² $0.09 \leq z \leq 1.965$ as summarized in Table 1 in [88].
- (BAO) The BAO data are provided by the SDSS Galaxy Consensus, quasars and Lyman- α forests [89] and the data from the DESI DR1 collaboration [90–92] where we refer as BAO₁ and the DESI DR2 collaboration [42–44] which we refer as BAO₂. These data sets provide observation values of the $\frac{D_M}{r_s}$, $\frac{D_V}{r_s}$, $\frac{D_H}{r_s}$ where r_s is the sound horizon at the drag epoch, D_M is the comoving angular distance $D_M = (1+z)^{-1} D_L$; D_V is the volume averaged distance $D_V^3 = c D_L \frac{z}{H(z)}$ and D_H is the Hubble distance $D_H = \frac{c}{H}$.

4.1. Methodology

In order to obtain the optimal values for the cosmological parameters we employ the Bayesian inference COBAYA³ [85, 86] with a custom theory and the MCMC sampler. From the results of the Planck 2018 collaborations [93] we consider the energy density for the radiation to be $\Omega_{r0} = 4.15 \cdot 10^{-5}$. Thus, we constrain our proposed models for the parameters $\{H_0, \Omega_{m0}, \mathbf{w}, r_{drag}\}$, where \mathbf{w} describes the vector of parameters within the equation of state parameters, as they are given in Table I and $\Omega_{m0} = \Omega_{dm0} + \Omega_{b0}$.

For all the runs we selected the priors $H_0 \in [60, 75]$, $\Omega_{m0} \in [0.2, 0.45]$ and $r_{drag} \in [130, 160]$.

The parameters in \mathbf{w} were assigned different ranges for each model, because their contributions vary due to the different functional forms of the dark energy models.

As the models under consideration have different dimension κ in their parameter space, we introduce the Akaike Information Criterion (AIC) to compare them statistically. The AIC, for Gaussian errors, is defined as

$$AIC = -2 \ln \mathcal{L}_{\max} + 2\kappa + \frac{2\kappa(\kappa - 1)}{N_{tot} - (\kappa + 1)},$$

where \mathcal{L}_{\max} is the maximum value for the likelihood and N_{tot} is the total number of data. For a large number of data the later formula is

$$AIC \simeq -2 \ln \mathcal{L}_{\max} + 2\kappa$$

Recall that for the combined data, the likelihood \mathcal{L}_{\max} is defined as

$$\mathcal{L}_{\max}^{total} = \mathcal{L}_{\max}^{SN} \times \mathcal{L}_{\max}^{CC} \times \mathcal{L}_{\max}^{BAO},$$

where $\mathcal{L}_{\max} = \exp(-\frac{1}{2}\chi_{\min}^2)$. The difference of the AIC parameters between two models

$$\Delta(AIC) = AIC_1 - AIC_2$$

gives information if the models are statistically indistinguishable. The higher the value of parameter ΔAIC , the higher the evidence against the model with higher value of AIC ; a difference $|\Delta AIC| > 2$ indicates a positive such evidence and $|\Delta AIC| > 6$ indicates a strong such evidence, while a value $|\Delta AIC| < 2$ indicates consistency among the two models in comparison.

5. RESULTS

We constrain the dynamical dark energy models using two sets of data: (I) Supernova and Cosmic Chronometers ($SN + CC$) and (II) Supernova, Cosmic Chronometers and Baryonic Acoustic Oscillations of DESI DR1 ($SN + CC +$

¹ <https://github.com/PantheonPlusSH0ES/DataRelease>

² https://github.com/Ahmadmehrabi/Cosmic_chronometer_data

³ <https://cobaya.readthedocs.io/>

BAO_1) and (III) Supernova, Cosmic Chronometers and Baryonic Acoustic Oscillations of DESI DR2 ($SN + CC + BAO_2$). We determine the free parameters along with their corresponding 1σ errors by locating the maximum of the likelihood functions. The results for the two tests are presented in Tables II, III and IV.

We consider the Λ CDM model as a reference theory. In Tables II, III and IV, we compute the parameter $\Delta(AIC)$ for each constraint to assess the statistical preference of the models based on the given datasets. We note that the models $w_{\pm}^I(z)$, $w^{II}(z)$ and $w_{\pm}^{IV}(z)$ introduce only one additional degree of freedom compared to Λ CDM, whereas the models $w^{III}(z)$, $w^V(z)$, and $w^{VI}(z)$ have two extra free parameters. In Figs. 2 and 3 we present the qualitative evolution of the dynamical dark energy parameters.

5.1. $SN + CC$ data

From the $SN + CC$ data, the Λ CDM model provides the maximum likelihood with the minimum value $\chi_{SN+CC}^2(\Lambda) = 1419.5$. The models $w_{\pm}^I(z)$ fit the data with similar values for the physical parameters, with best-fit values $w_a^{I-} = -0.24$ and $w_a^{I+} = -0.05$, and a corresponding chi-square value of $\chi_{SN+CC}^2(w_+^I) = 1419.8$ and $\chi_{SN+CC}^2(w_+^I) = 1419.9$. Thus, the difference in the Akaike Information Criterion (AIC) compared to Λ CDM are $\Delta(AIC) = 2.3$ and 2.4 respectively.

For model $w^{II}(z)$, the best-fit value is $w_a = -0.37$, with a minimum chi-square value of $\chi_{SN+CC}^2(w^{II}) = 1419.9$, leading to $\Delta(AIC) = 2.4$. On the other hand, for model $w^{III}(z)$, we search for the best-fit values within the ranges $w_a \in [-30, 10]$ and $w_b \in [-5, 5]$. The analysis indicates that the two variables are degenerate, as previously discussed. Nevertheless, within this range, we find that $w_a < -12.6$ and $w_b = 1.1$, with $\chi_{SN+CC}^2(w^{III}) = 1419.7$ and $\Delta(AIC) = 4.2$.

For the models of the second parametrization, we consider the parameter ranges $w_a \in (0, 30]$ and $w_b \in [0, 30]$ or $w_b \in [-10, 10]$. However, this dataset is not sufficient to fully constrain the free parameters of this family of models. For models $w_{\pm}^{IV}(z)$, we find that $w_a > 6.6$ and $w_a = 10.1$, respectively, which are relatively large values, in agreement with the analysis presented previously in [82]. The likelihood reaches its maximum value with $\chi_{SN+CC}^2(w_+^{IV}) = 1419.7$ and $\chi_{SN+CC}^2(w_+^{IV}) = 1419.5$, resulting in $\Delta(AIC) = 2.2$ and 2.0 respectively.

Moreover, models $w^V(z)$ and $w^{VI}(z)$ fit the data with similar values of χ_{SN+CC}^2 ; however, due to the larger number of degrees of freedom, their corresponding $\Delta(AIC)$ values are higher. For model $w^{VI}(z)$, it is important to note that the parameter w_b could not be constrained at all, indicating a strong correlation between the free parameters.

These results are summarized in Table II.

According to the AIC, for the SN+CC data, the models Λ CDM and w_{\pm}^{IV} are statistically indistinguishable. Additionally, there is strong evidence that the models $w^{III}(z)$, $w^V(z)$ and $w^{VI}(z)$ do not fit the data as well as Λ CDM.

The key conclusion from this analysis is that this dataset alone cannot effectively distinguish between the models. This implies that, near the present time, all asymptotic-like behaviors remain viable. However, in this study, we utilized SN data with $z > 1$, meaning that these models are not merely considered as asymptotic solutions but rather as representations of the general behavior of the equation of state parameter, as dictated by a linear second-order differential equation.

5.2. DESI DR1: $SN + CC + BAO_1$ data

We perform a constraint on these models by additionally incorporating BAO_1 data. The maximum likelihood value is again provided by the Λ CDM model, with $\chi_{\min}^2(\Lambda) = 1435.2$. The models $w_{\pm}^I(z)$ fit the data with $\chi_{\min}^2(w_+^I) = 1435.8$ and $\chi_{\min}^2(w_-^I) = 1435.4$, respectively. However, due to the different number of free parameters, the corresponding $\Delta(AIC)$ values are 2.6 and 2.2 , respectively.

On the other hand, model $w^{II}(z)$ fits the data with the same maximum likelihood value, that is, $\chi_{\min}^2(w^{II}) = 1435.4$, leading to $\Delta(AIC) = 2.2$. Moreover, for $w^{III}(z)$, we find $\chi_{\min}^2(w^{III}) = 1433.5$, with $\Delta(AIC) = 2.3$.

For all these models, the best-fit parameters remain within 1σ in comparison with the previous test without BAO data. A particularly interesting result is that, when BAO data are included, model $w^{III}(z)$ has a lower $\Delta(AIC)$ value, contrary to the results from the SN+CC dataset. Meanwhile, model $w_+^{IV}(z)$ provides the same $\Delta(AIC)$ value as in the previous test.

We continue with the second family of models, which follows from the logarithmic parametrization. These models do not fit the cosmological data in the same way. The corresponding values for χ_{\min}^2 are $\chi_{\min}^2(w_+^{IV}) = 1435.3$, $\chi_{\min}^2(w_-^{IV}) = 1434.8$, $\chi_{\min}^2(w^V) = 1435.3$ and $\chi_{\min}^2(w^{VI}) = 1435.0$. Thus, for the models w_{\pm}^{IV} , we calculate

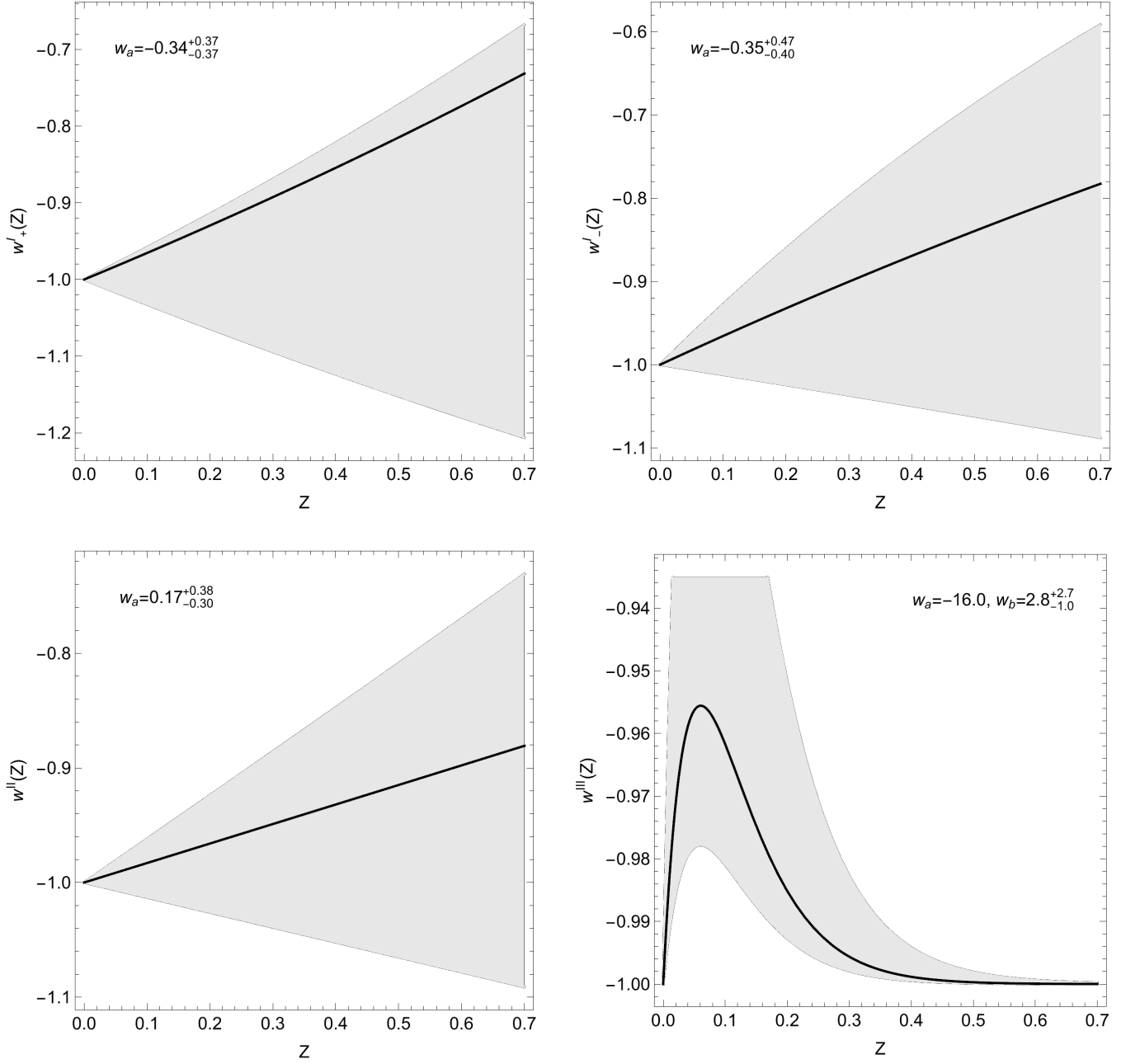


FIG. 2: Evolution for the dark energy equation of state parameter $w_{\pm}^I(z)$, $w^{II}(z)$ and $w^{III}(z)$.

$\Delta(AIC) \leq 2$, indicating that these models are statistically equivalent to the Λ CDM model. The results are summarized in Table III.

When BAO_1 data are introduced, models $w_{\pm}^{IV}(z)$ and $w^{VI}(z)$ lead to a smaller value of $\Delta(AIC)$ in comparison to the Λ CDM model. However, this is not the case for model $w^V(z)$. We note that the parameters of model $w^{VI}(z)$ cannot be constrained by the data analysis. Models $w^V(z)$ and $w^{VI}(z)$ are ruled out by these cosmological data.

5.3. DESI DR2: $SN + CC + \text{BAO}_2$ data

We introduce the BAO_2 data as given by the DESI DR2 and we perform the same analysis. We show that for these models there is not any difference between the BAO_1 and BAO_2 data in terms of the χ^2_{\min} or the $\Delta(AIC)$. Λ CDM fits the data in a better way with the rest of the models. However, there is small statistical preference on the

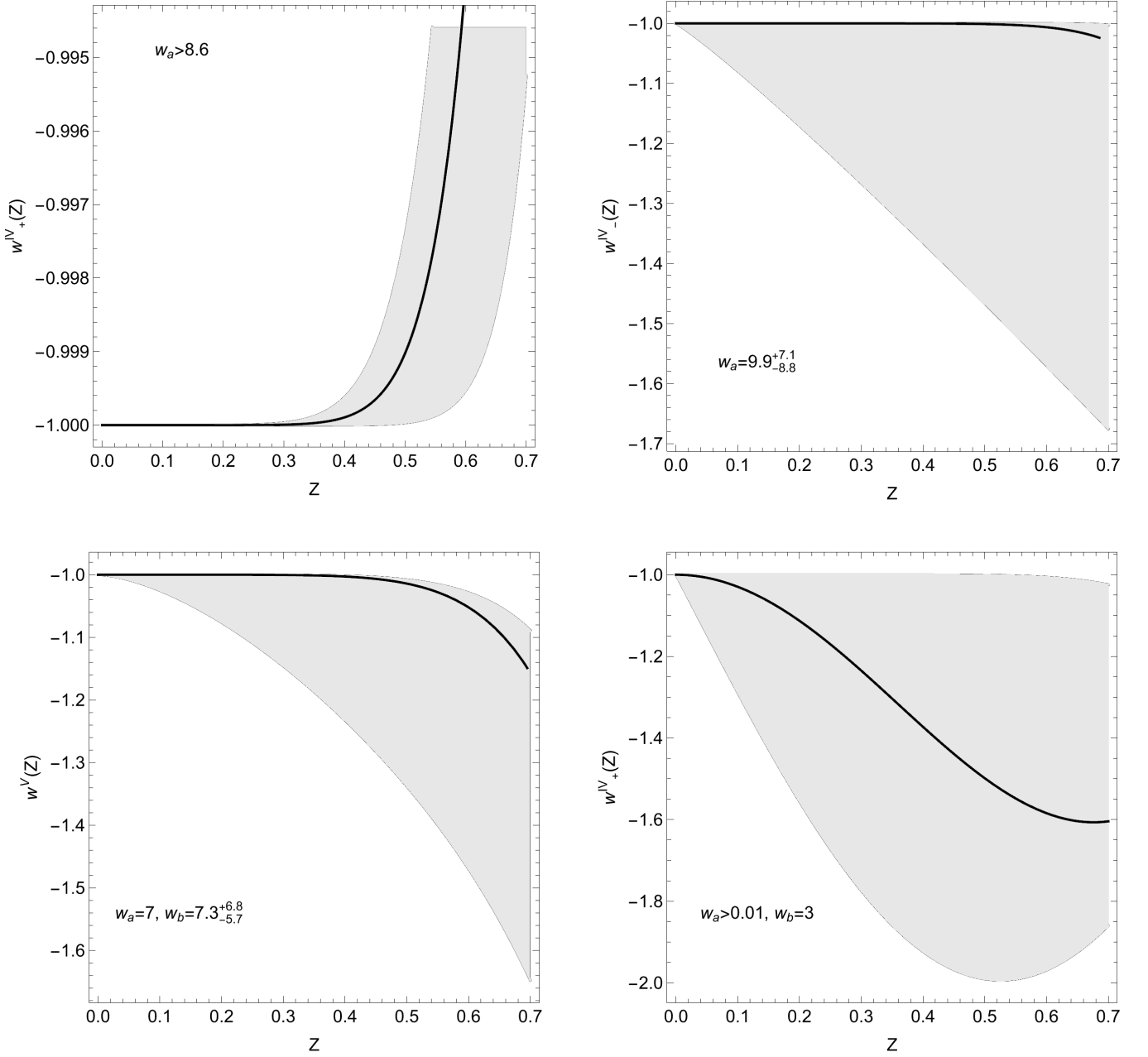


FIG. 3: Evolution for the dark energy equation of state parameter $w_{\pm}^{IV}(z), w^V(z)$ and $w^{VI}(z)$.

Λ CDM in comparison with the rest of the parametric dark energy models.

In Figs. 4, 5 and 6 we present the contour plots for the 1σ values of the best fit parameters for models $w_{\pm}^I(z), w^{II}(z), w^{III}(z)$ and $w_{\pm}^{IV}(z)$ for the data sets $SN + CC$ and $SN + CC + BAO_2$.

6. CONCLUSIONS

In this work, we considered that the equation of state parameter for dark energy is described by an arbitrary autonomous second-order differential equation, with the cosmological constant as an equilibrium point. We derived three functional forms for the asymptotic solutions of this differential equation, describing the behavior of the equation of state parameter near the equilibrium point. The free parameters of these functions depend upon the initial value problem and the eigenvalues of the linearized differential equation in the vicinity of the equilibrium point. Thus,

TABLE II: Constraints for the $SN + CC$ data.

Model	H_0	Ω_{m0}	w_a	w_b	χ^2_{\min}	$AIC - AIC_\Lambda$
Λ CDM	$67.5^{+1.6}_{-1.9}$	$0.331^{+0.017}_{-0.017}$	\nexists	\nexists	1419.5	0
$w^I_+(z)$	$67.5^{+1.7}_{-1.7}$	$0.337^{+0.049}_{-0.025}$	$-0.24^{+0.76}_{-0.66}$	\nexists	1419.8	2.3
$w^I_-(z)$	$67.7^{+1.8}_{-1.8}$	$0.324^{+0.063}_{-0.032}$	$-0.05^{+0.74}_{-0.74}$	\nexists	1419.9	2.4
$w^{II}(z)$	$67.5^{+1.8}_{-1.8}$	$0.345^{+0.052}_{-0.038}$	$-0.37^{+1.1}_{-0.65}$	\nexists	1419.9	2.4
$w^{III}(z)$	$67.7^{+1.7}_{-1.9}$	$0.327^{+0.029}_{-0.029}$	< -12.6	$1.1^{+2.6}_{-2.6}$	1419.7	4.2
$w^{IV}_+(z)$	$67.6^{+1.8}_{-1.8}$	$0.328^{+0.022}_{-0.017}$	> 6.6	\nexists	1419.7	2.2
$w^{IV}_-(z)$	$67.7^{+1.7}_{-1.7}$	$0.333^{+0.018}_{-0.020}$	$10.1^{+6.4}_{-8.3}$	\nexists	1419.5	2.0
$w^V(z)$	$67.7^{+1.7}_{-1.7}$	$0.331^{+0.024}_{-0.024}$	> 5.63	> 4.92	1419.5	4.0
$w^{VI}(z)$	$67.8^{+1.7}_{-1.7}$	$0.326^{+0.019}_{-0.010}$	$15.7^{+8.3}_{-8.3}$	—	1419.2	3.7

TABLE III: Constraints for the $SN + CC + BAO_1$ data.

Model	H_0	Ω_{m0}	w_a	w_b	χ^2_{\min}	$AIC - AIC_\Lambda$
Λ CDM	$68.8^{+1.2}_{-1.7}$	$0.311^{+0.012}_{-0.012}$	\nexists	\nexists	1435.2	0
$w^I_+(z)$	$68.7^{+1.2}_{-1.6}$	$0.303^{+0.024}_{-0.018}$	$0.09^{+0.39}_{-0.27}$	\nexists	1435.8	2.6
$w^I_-(z)$	$68.8^{+1.2}_{-1.6}$	$0.293^{+0.028}_{-0.019}$	$-0.34^{+0.47}_{-0.36}$	\nexists	1435.4	2.2
$w^{II}(z)$	$68.8^{+1.2}_{-1.6}$	$0.298^{+0.029}_{-0.017}$	$0.20^{+0.37}_{-0.37}$	\nexists	1435.8	2.6
$w^{III}(z)$	$68.7^{+1.2}_{-1.2}$	$0.307^{+0.012}_{-0.012}$	$-17.1^{+6.8}_{-9.0}$	> 1.57	1433.5	2.3
$w^{IV}_+(z)$	$68.6^{+1.3}_{-1.5}$	$0.310^{+0.012}_{-0.012}$	$11.3^{+4.8}_{-4.8}$	\nexists	1435.3	2
$w^{IV}_-(z)$	$68.6^{+1.4}_{-1.4}$	$0.313^{+0.012}_{-0.012}$	$9.8^{+6.6}_{-7.7}$	\nexists	1434.8	1.6
$w^V(z)$	$68.5^{+1.6}_{-1.6}$	$0.310^{+0.014}_{-0.014}$	> 5.81	> 3.90	1435.3	4.1
$w^{VI}(z)$	$69.1^{+1.2}_{-1.5}$	$0.312^{+0.012}_{-0.012}$	—	—	1435.0	3.8

TABLE IV: Constraints for the $SN + CC + BAO_2$ data.

Model	H_0	Ω_{m0}	w_a	w_b	χ^2_{\min}	$AIC - AIC_\Lambda$
Λ CDM	$68.9^{+1.2}_{-1.5}$	$0.311^{+0.012}_{-0.012}$	\nexists	\nexists	1435.1	0
$w^I_+(z)$	$68.8^{+1.2}_{-1.5}$	$0.303^{+0.023}_{-0.018}$	$0.12^{+0.35}_{-0.28}$	\nexists	1435.7	2.6
$w^I_-(z)$	$68.8^{+1.2}_{-1.6}$	$0.293^{+0.031}_{-0.020}$	$-0.33^{+0.51}_{-0.42}$	\nexists	1435.8	2.7
$w^{II}(z)$	$68.8^{+1.3}_{-1.6}$	$0.296^{+0.028}_{-0.019}$	$0.25^{+0.35}_{-0.35}$	\nexists	1435.9	2.8
$w^{III}(z)$	$68.6^{+1.0}_{-1.4}$	$0.308^{+0.012}_{-0.012}$	$-17.1^{+7.2}_{-8.5}$	$2.6^{+2.9}_{-1.5}$	1433.4	2.3
$w^{IV}_+(z)$	$68.6^{+1.3}_{-1.5}$	$0.310^{+0.012}_{-0.012}$	> 7.61	\nexists	1435.3	2.1
$w^{IV}_-(z)$	$68.8^{+1.4}_{-1.4}$	$0.313^{+0.012}_{-0.012}$	$9.1^{+3.1}_{-7.3}$	\nexists	1434.9	1.8
$w^V(z)$	$68.5^{+1.7}_{-1.7}$	$0.312^{+0.014}_{-0.014}$	> 6.65	> 4.39	1435.4	4.3
$w^{VI}(z)$	$68.9^{+1.2}_{-1.4}$	$0.311^{+0.012}_{-0.012}$	$14.5^{+8.5}_{-8.5}$	> -2.84	1434.7	3.6

TABLE V: Constraints for the $SN + CC + BAO_2$ data of modified CPL models.

Model	H_0	Ω_{m0}	w_0	w_a	w_b	χ^2_{\min}	$AIC - AIC_{CPL}$	$AIC - AIC_{\Lambda}$
CPL	$68.4^{+1.1}_{-1.4}$	$0.308^{+0.021}_{-0.015}$	$-0.893^{+0.056}_{-0.056}$	$-0.33^{+0.43}_{-0.48}$	$\#$	1433.3	0	2.2
$\hat{w}_+^I(z)$	$68.2^{+1.2}_{-1.4}$	$0.301^{+0.026}_{-0.012}$	$-0.894^{+0.057}_{-0.057}$	$-0.26^{+0.26}_{-0.74}$	$\#$	1433.4	0.1	2.3
$\hat{w}_-^I(z)$	$68.3^{+1.2}_{-1.4}$	$0.303^{+0.028}_{-0.016}$	$-0.906^{+0.060}_{-0.060}$	$0.17^{+0.65}_{-0.36}$	$\#$	1433.6	0.3	2.5
$\hat{w}^{II}(z)$	$68.4^{+1.1}_{-1.4}$	$0.311^{+0.021}_{-0.017}$	$-0.885^{+0.061}_{-0.061}$	$-0.43^{+0.56}_{-0.42}$	$\#$	1433.5	0.2	2.4
$\hat{w}^{III}(z)$	$68.3^{+1.1}_{-1.1}$	$0.300^{+0.013}_{-0.013}$	$-0.993^{+0.042}_{-0.056}$	< 16.9	$0.98^{+4.8}_{-4.3}$	1433.2	1.9	4.1
$\hat{w}_+^{IV}(z)$	$68.3^{+1.2}_{-1.2}$	$0.295^{+0.017}_{-0.013}$	$-0.914^{+0.044}_{-0.053}$	> 7.4	$\#$	1433.1	-0.2	2.0
$\hat{w}_-^{IV}(z)$	$68.4^{+1.2}_{-1.2}$	$0.302^{+0.015}_{-0.015}$	$-0.922^{+0.040}_{-0.051}$	> 6.7	$\#$	1433.1	-0.2	2.0
$\hat{w}^V(z)$	$68.0^{+1.6}_{-1.6}$	$0.298^{+0.018}_{-0.015}$	$-0.916^{+0.044}_{-0.053}$	> 5.6	$7.4^{+3.0}_{-6.1}$	1433.8	2.5	4.7
$\hat{w}^{VI}(z)$	$68.4^{+1.1}_{-1.4}$	$0.299^{+0.042}_{-0.050}$	$-0.920^{+0.042}_{-0.050}$	16^{+14}_{-11}	-	1433.2	1.9	4.1

constraining these parameters provides important insights into the physical properties that the equation of state parameter must satisfy. Based on these asymptotic solutions, we constructed families of dynamical dark energy models.

We considered two families of models based on the parametrization of the differential equation, each consisting of four models. The first family follows from the linear parametrization of the equation of state parameter with respect to the scale factor, while the second family follows from the logarithmic parametrization of the equation of state parameter with respect to the scale factor. By analyzing the parameter space of the free variables, we were able to reduce the number of dependent variables to a maximum of two. These parameters were then constrained using observational cosmological data, specifically the Supernova, Cosmic Chronometers, and Baryon Acoustic Oscillation datasets.

For the first family of models, which includes, $w_{\pm}^I(z)$, $w^{II}(z)$ and $w^{III}(z)$, by using the Supernova and Cosmic Chronometers, we found that the Λ CDM cosmology remains the statistical preferred model. However, $w^{III}(z)$, which described oscillations, has a strong degeneracy in the free parameters. Nevertheless, when then BAO data are introduced, models $w^{II}(z)$ and $w^{III}(z)$ provide a better fit, although Λ CDM remains the preferred model.

On the other hand, for the second family of models, which follows from the logarithmic parametrization, we found that $w_{\pm}^{IV}(z)$ models are statistically equivalent to Λ CDM with $\Delta(AIC) \leq 2$. However, models $w^V(z)$ and $w^{VI}(z)$ were strongly disfavored by the data. The parameters of model $w^V(z)$ could not be constrained, which means that there exists a high degree of correlation in the parameter space.

In the case for which the equilibrium point is not the Λ CDM model but a constant value w_0 , we can introduce a new class of models

$$\hat{w}^A(z) = (1 + w_0) + w^A(z) ,$$

with $A = I, II, III, \dots$, where at the present time $\hat{w}^A(z \rightarrow 0) = w_0$. These dynamical dark energy models contain two or three free parameters. We apply the same observational constraints as before, but now using the CPL model as a reference. The combination of observational data yields the best-fit parameters summarized in Table V. In Fig. 7, we present the evolution of the equation of state parameters $w^A(z)$ for the best-fit parameters of Table V.

We observe that most models fit the observational data with a χ^2_{\min} value smaller than that of CPL and Λ CDM. However, due to the different number of degrees of freedom, the application of the AIC indicates that, in comparison to CPL, the models $\hat{w}^A(z)$ are statistically indistinguishable. The best fit is provided by $\hat{w}_-^{IV}(z)$, which is known as the n CPL model. Finally, if when we compare the results of Table IV and V, we conclude that the DESI DR2 BAO data support models with $w_0 > -1$.

Although these models have been introduced to describe the asymptotic behavior of $w(z)$ near the equilibrium point at the present time, our analysis shows that these models can be used for observational constraints in the late universe. However, for CMB data, where $z \gg 1$, we show that the free parameters are degenerate, and this approximation may not be valid.

This consideration is different from the Taylor expansion of the $w(a)$ around the present time. Indeed, the CPL can be seen as the first-order approximation of a nonlinear $w(z)$ in the Taylor expansion. The introduction of additional terms in the Taylor expansion is done with the charge of additional free parameters. This can lead to new problems

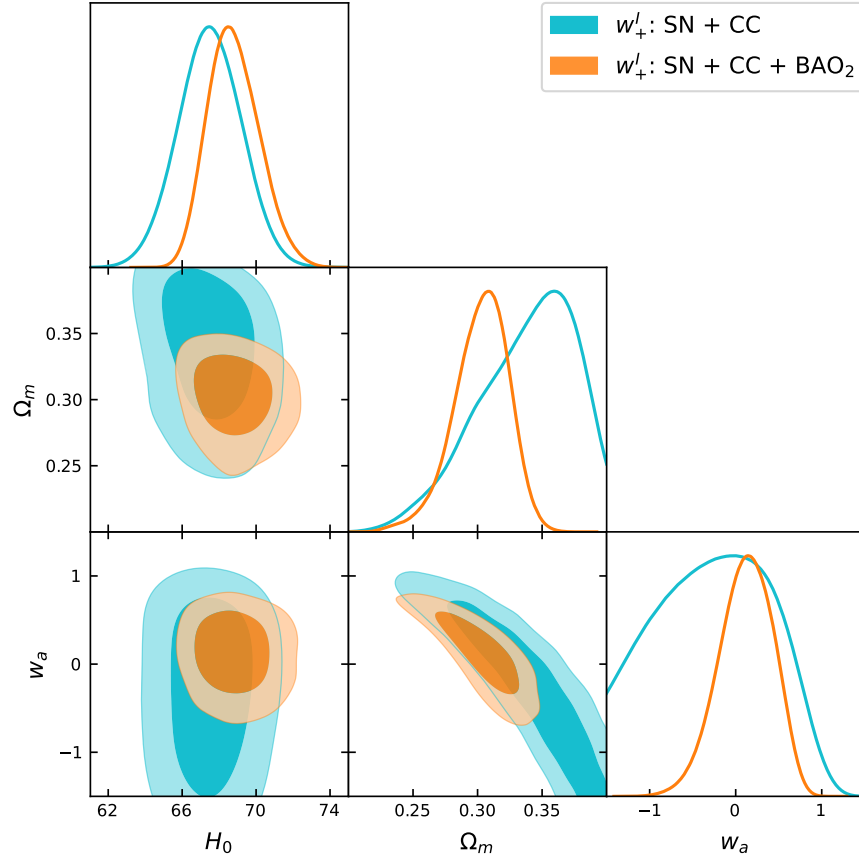
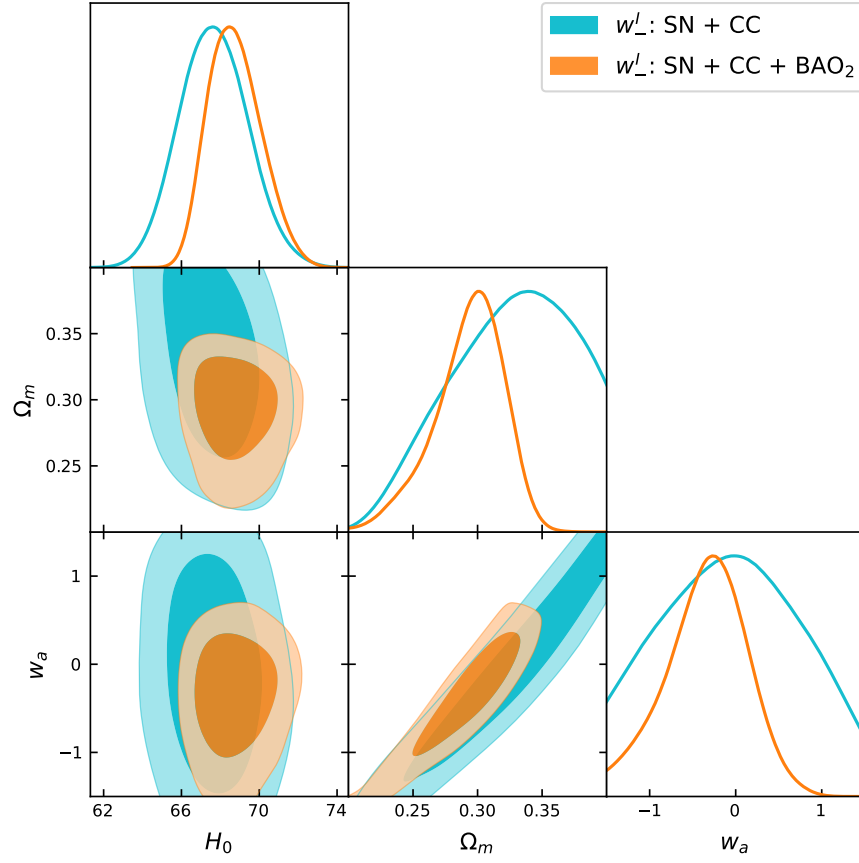
as discussed recently in [55]. However, in our approach we can reconstructing the asymptotic behavior of $w(z)$ at different epochs. This can lead to further constrain to the physical law that $w(z)$ satisfies. In turn, can provide important insights into the nature of dark energy. From this work it follows that the logarithmic parametrization leads to parametric dark energy models which fit the data in a better way. Moreover, the existence of oscillations, i.e. model $\hat{w}^{VI}(z)$, lead to smaller values of the χ^2_{\min} , with the cost of a greater value for the AIC due to the larger number of free parameters. We recall that the Chiral multi-scalar field theory [94–97], known as warm inflation [98], provide such oscillating behaviours.

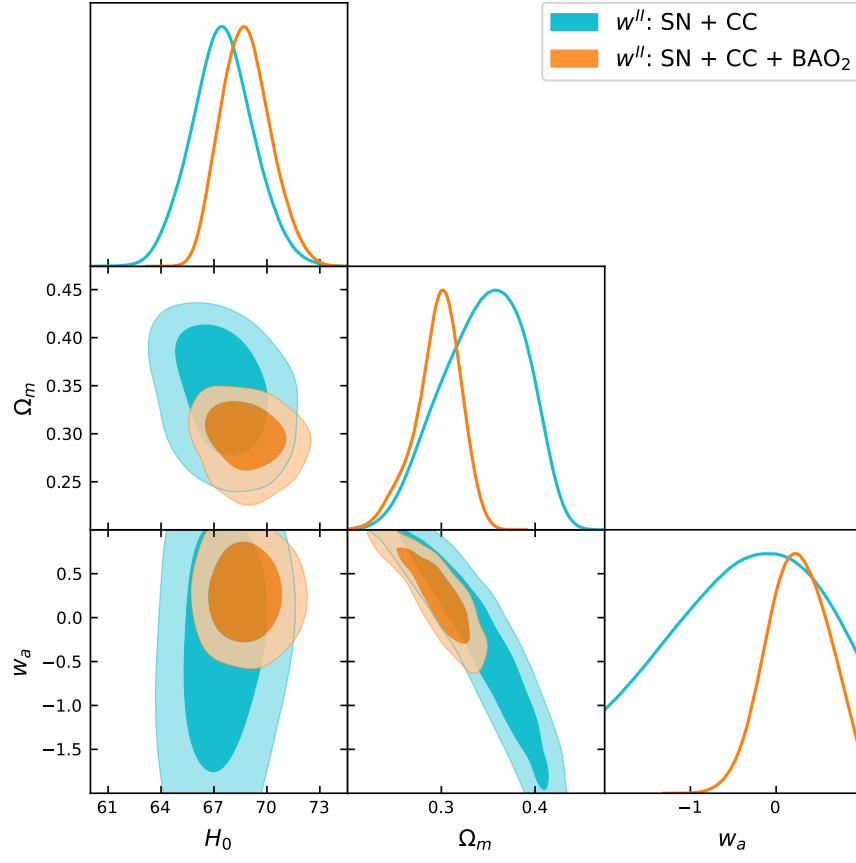
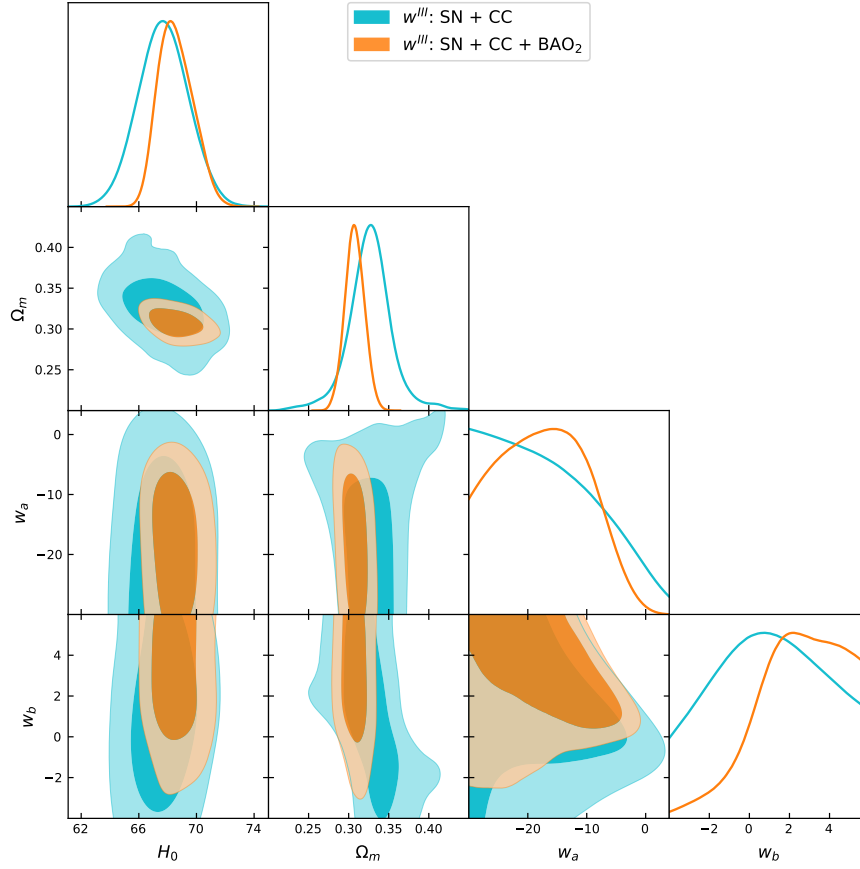
Acknowledgments

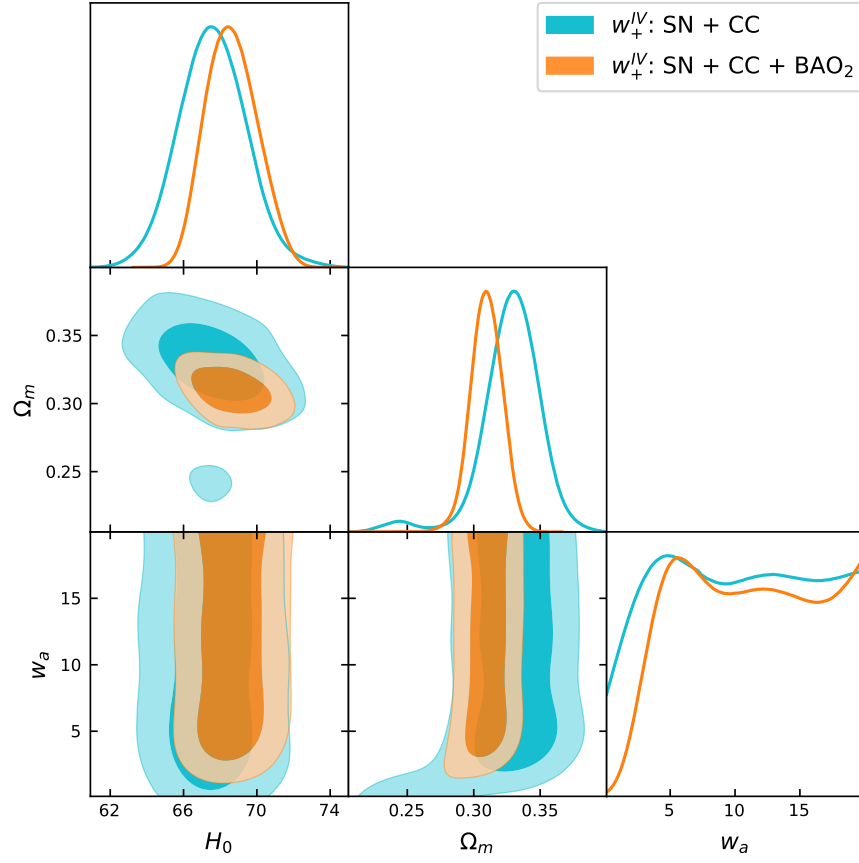
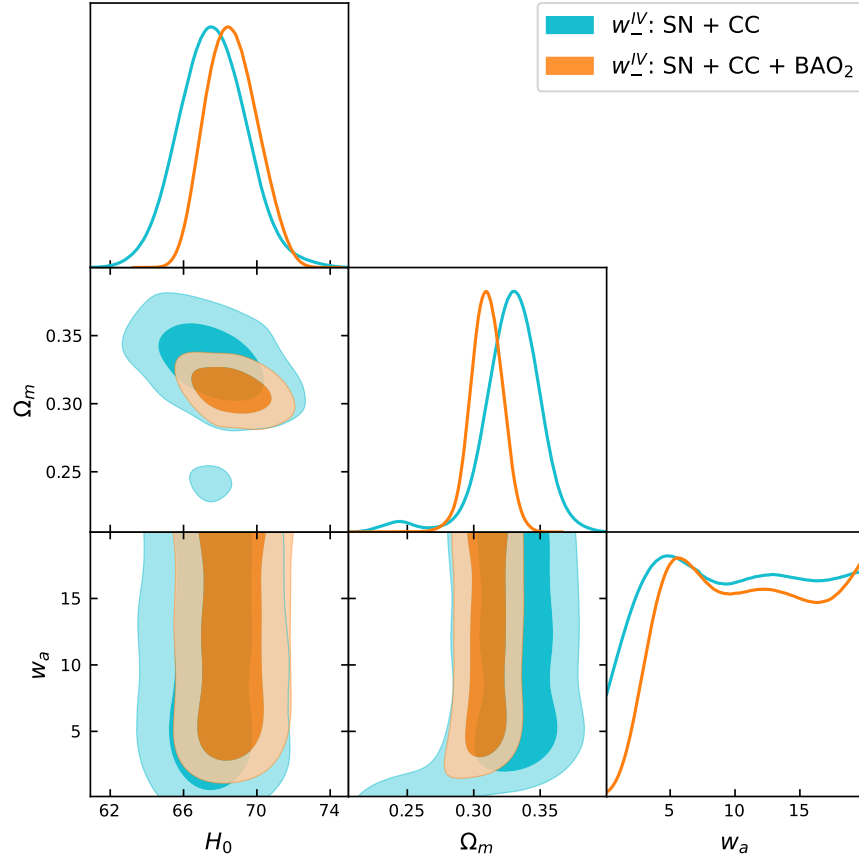
AP thanks the support of VRIDT through Resolución VRIDT No. 096/2022 and Resolución VRIDT No. 098/2022. Part of this study was supported by FONDECYT 1240514 Etapa 2025. AP thanks Dr. F. Anagnostopoulos for a fruitful discussion.

-
- [1] A.G. Riess et al., *Astron. J.* 116, 1009 (1998)
 - [2] M. Tegmark et al., *Astrophys. J.* 606, 702 (2004)
 - [3] M. Kowalski et al., *Astrophys. J.* 686, 749 (2008)
 - [4] E. Komatsu et al., *Astrophys. J. Suppl. Ser.* 180, 330 (2009)
 - [5] N. Suzuki et al., *Astrophys. J.* 746, 85 (2012)
 - [6] J. Yoo and Y. Watanabe, *Int. J. Mod. Phys. D* 21, 1230002 (2012)
 - [7] G. Gutierrez, *Nucl. Part. Phys. Proceedings*, 267, 332 (2015)
 - [8] K. Bamba, *LHEP* 2022, 352 (2022)
 - [9] S. Weinberg, *Rev. Mod. Phys.* 61, 1 (1989)
 - [10] T. Padmanabhan, *Phys. Rept.* 380, 235 (2003)
 - [11] L. Perivolaropoulos, (2008) [arXiv:0811.4684](#)
 - [12] L. Perivolaropoulos and F. Skara, *New Astron. Rev.* 95, 101659 (2022)
 - [13] E. Di Valentino et al., *Atropharticle Physics* 131, 102605 (2021)
 - [14] E. Abdalla et al., *JHEAp* 34, 49 (2022)
 - [15] P.K.S. Dunby, O. Luongo and L. Reverberi, *Phys. Rev. D* 94, 083525 (2016)
 - [16] D. Benisty, E.I. Guendelman, A. van de Venn, D. Vasak, J. Struckmeier and H. Stoecker, *Eur. Phys. J C* 82, 264 (2022)
 - [17] A. Joyce, L. Lombriser and F. Schmidt, *Annu. Rev. Nucl. Part Sci.* 66, 95 (2016)
 - [18] S. Tsujikawa, *Lect. Notes Phys.* 800, 2010
 - [19] O. Luongo and D. Tommasini, *Int. J. Mod. Phys. D* 23, 1450023 (2014)
 - [20] Y. Carloni and O. Luongo, [arXiv:2410.10935](#)
 - [21] F.K. Anagnostopoulos, A. Bonanno, A. Mitsa and V. Zarikas, *Phys. Rev. D* 105, 083532 (2022)
 - [22] F.K. Anagnostopoulos and E.N. Saridakis, *JCAP* 04, 051 (2024)
 - [23] Y. Qi, W. Yang, Y. Wang, T. Han and Y. Wu, *Eur. Phys. J. C* 84, 415 (2024)
 - [24] S.D. Odintsov, V.K. Oikonomou and F.P. Fronimos, *Class. Quantum Grav.* 38, 075009 (2021)
 - [25] S.D. Odintsov and V.K. Oikonomou, *Phys. Rev. D* 104, 124065 (2021)
 - [26] A. Paliathanasis, *Phys. Dark. Univ.* 41, 101255 (2023)
 - [27] A. Aviles, L. Bonanno, O. Luongo and H. Quevedo, *Phys. Rev. D* 84, 103520 (2011)
 - [28] A. Belfiglio, R. Giambo, O. Luongo and Al Karbi Kazakh, *Class. Quantum Grav.* 40, 105004 (2023)
 - [29] Y. Carloni and O. Luongo, *Eur. Phys. J. C* 84, 519 (2024)
 - [30] G. Efstathiou, *MNRAS* 310, 842 (1999)
 - [31] J. Weller and A. Albrecht, *Phys. Rev. Lett.* 86, 1939 (2001)
 - [32] L. Feng and T. Lu, *JCAP* 11, 034 (2011)
 - [33] C. Valelis, F.K. Anagnostopoulos, S. Basilakos and E.N. Saridakis, *Int. J. Mod. Phys. D* 30, 2150085 (2021)
 - [34] F.K. Anagnostopoulos and S. Basilakos, *Phys. Rev. D* 97, 063503 (2018)
 - [35] O. Luongo, G.B. Pisani and A. Troisi, *Int. J. Mod. Phys. D* 26, 1750015 (2016)
 - [36] M. Chevallier and D. Polarski, *Int. J. Mod. Phys. D* 10, 213 (2001)
 - [37] E.V. Linder, *Phys. Rev. Lett.* 90, 091301 (2003)
 - [38] A. Shafiello, V. Sahni and A. Starobinsky, *Annalen Phys.* 19, 316 (2010)
 - [39] W. Giarè T. Mahassen, E. Di Valentino and S. Pan, [arXiv:2502.10264](#)
 - [40] W. Giarè, M. Najadi, S. Pan, E. Di Valentino and J.T. Firouzjaee, *JCAP* 10, 035 (2024)
 - [41] Y. Carloni and O. Luongo, *Phys. Rev. D* 111, 023512 (2025)
 - [42] DESI Collaboration: M.A. Karim et al. (2025) [[arXiv:2503.14739](#)]
 - [43] DESI Collaboration: M.A. Karim et al. (2025) [[arXiv:2503.14738](#)]
 - [44] DESI Collaboration: K. Lodha et al. (2025) [[arXiv:2503.14743](#)]

- [45] E. Silva, M. A. Sabogal, M. S. Souza, R. C. Nunes, E. Di Valentino, and S. Kumar (2025), arXiv: 2503.23225
- [46] Y. Yang, Q. Wang, X. Ren, E. N. Saridakis, and Y.-F. Cai (2025), arXiv: 2504.06784
- [47] A. Paliathanasis (2025), arXiv: 2503.20896
- [48] A. Paliathanasis (2025), arXiv: 2504.11132
- [49] G.G. Luciano, A. Paliathanasis and E.N. Saridakis (2025), arXiv: 2504.12205
- [50] F. B. M. d. Santos, J. Morais, S. Pan, W. Yang, and E. Di Valentino (2025), arXiv: 2504.04646
- [51] C. You, D. Wang, and T. Yang (2025), arXiv: 2504.00985
- [52] G. Ye and Y. Cai (2025), arXiv: 2503.22515
- [53] R. Shah, P. Mukherjee, and S. Pal (2025), arXiv: 2503.21652
- [54] E. Specogna, S.A. Adil, E. Ozulker, E. Di Valentino and R.C. Nunes (2025), arXiv: 2504.17859
- [55] S. Nesseris, Y. Akrami and G.D. Starkman (2025), arXiv: 2503.22529
- [56] S. Afroz and S. Mukherjee (2025), arXiv: 2504.16868
- [57] S. Pan, S. Paul, E.N. Saridakis and W. Yang (2025), arXiv: 2504.00994
- [58] S.R. Choudhury (2025), arXiv:2504.15340
- [59] M. Rezaei, M. Malekjani, S. Basilakos, A. Mehrabi, and D. F. Mota, *Astrophys. J.* 843, 65 (2017)
- [60] J.-Z. Ma and X. Zhang, *Phys. Lett. B* 699, 233 (2011)
- [61] L. Xing, J. Chen, Y. Gui, E. Schlegel and J. Lu, *Mod. Phys. Lett. A* 26, 885 (2011)
- [62] E.M. Barboza Jr. and J.S. Alcaniz, *Phys. Lett. B* 666, 415 (2008)
- [63] R.C. Bernardo, D. Grandon, J.L Said and V.H. Cardenas, *Phys. Dark Univ.* 36, 101017 (2022)
- [64] S. Nesseris and L. Perivolaropoulos, *Phys. Rev. D* 70, 043531 (2004)
- [65] N. Dimakis, A. Karagiorgos, A. Zampeli, A. Paliathanasis, T. Christodoulakis and Petros A. Terzis, *Phys. Rev. D* 93, 123518 (2016)
- [66] S. Pan, W. Yang and A. Paliathanasis, *Eur. Phys. J. C* 80, 274 (2020)
- [67] E.V. Linder, *Astropart. Phys.* 25, 167 (2006)
- [68] B. Feng, M. Li, Y.-S. Piao and X. Zhang, *Phys. Lett. B* 634, 101 (2006)
- [69] S. Pan, E.N. Saridakis and W. Yang, *Phys. Rev. D* 98, 063510 (2018)
- [70] M. Rezaei, *Astroph. J.* 967, 2 (2024)
- [71] L.A. Escamilla, S. Pan, E. Di Valentino, A. Paliathanasis and J.A. Vazquez, *Phys. Rev. D* 111, 2 (2025)
- [72] E.O. Colgain, M.M. Sheikh-Jabbari and L. Yin, *Phys. Rev. D* 104, 023510 (2021)
- [73] E.J. Copeland, A.R. Liddle and D. Wands, *Phys. Rev. D* 57, 4686 (1998)
- [74] R. Lazkoz and G. Leon, *Phys. Lett. B* 638, 303 (2006)
- [75] A. Paliathanasis, *Class. Quantum Grav.* 37, 19 (2020)
- [76] G. Leon, *Class. Quantum Grav.* 26, 035008 (2009)
- [77] A. Stachowski and M. Szydlowski, *Eur. Phys. J. C* 76, 606 (2016)
- [78] G. Caldera-Cabral, R. Maartens and L.A. Urena-Lopez, *Phys. Rev. D* 79, 063518 (2009)
- [79] J.D. Barrow and A. Paliathanasis, *Gen. Rel. Gravit.* 50, 82 (2018)
- [80] A. Paliathanasis, *Mod. Phys. Lett. A* 37, 2250119 (2022)
- [81] S.H. Strogatz, *Nonlinear Dynamics and Chaos*, CRC Press, Taylor and Francis Group (2018)
- [82] G. Pantazis, S. Nesseris and L. Perivolaropoulos, *Phys. Rev. D* 93, 103503 (2016)
- [83] D. Scolnic et al. *Astrophys. J.* 938, 113 (2022)
- [84] S. Alam, *Phys. Rev. D* 103, 083533 (2021)
- [85] J. Torrado and A. Lewis, *ascl:1910.019* (2019)
- [86] J. Torrado and A. Lewis, *JCAP* 05, 057 (2021)
- [87] D. Scolnic et al., *Ap. J.* 931, 113 (2022)
- [88] S. Vagnozzi, A. Loeb and M. Moresco, *Astrophys. J.* 908, 84 (2021)
- [89] eBOSS Collaboration: S. Alam, *Phys. Rev. D* 103, 083533 (2021)
- [90] DESI Collaboration: A. G. Adame [arXiv:2404.03000]
- [91] DESI Collaboration: A. G. Adame [arXiv:2404.03001]
- [92] DESI Collaboration: A. G. Adame [arXiv:2404.03002]
- [93] Planck Collaboration: N. Aghanim et al., *A&A* 641, A6 (2020)
- [94] A. Paliathanasis, *Gen. Rel. Grav.* 51, 106 (2019)
- [95] A. Paliathanasis, *Class. Quantum Grav.* 37, 19 (2020)
- [96] P. Christodoulidis and A. Paliathanasis, *JCAP* 05, 038 (2021)
- [97] S.V. Chervon, *Quantum Matter* 2, 71 (2013)
- [98] R. D' Agostino and O. Luongo, *Phys. Lett. B* 829, 137070 (2022)

(a) Contour plots for w_+^I (b) Contour plots for w_-^I FIG. 4: Contour plots for w_+^I & w_-^I

(a) Contour plots for w^{II} (b) Contour plots for w^{III} FIG. 5: Contour plots for w^{II} & w^{III}

(a) Contour plots for w_+^{IV} (b) Contour plots for w_-^{IV} FIG. 6: Contour plots for w_+^{IV} & w_-^{IV}

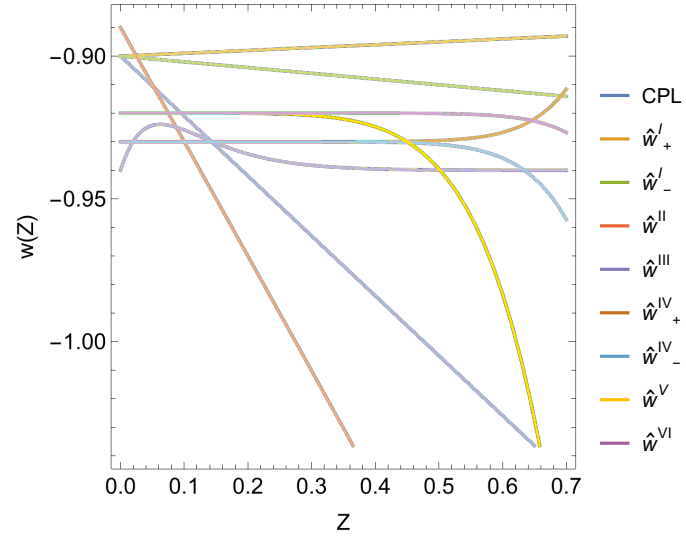


FIG. 7: Evolution for the dark energy equation of state parameter models: CPL, and \hat{w}^A for the best fit values of Table V.